Signatures of Temperature-Driven Lifshitz Transition in Semimetal Hafnium Ditelluride

Qixuan Li(黎绮镟)[1], Bin Wang(王彬)[1], Nannan Tang(唐喃喃)[1], Chushan Li(李楚善)[1], Enkui Yi(易恩魁)[1], Bing Shen(沈冰)[1], Donghui Guo(郭东辉)[1], Dingyong Zhong(钟定永)[2], and Huichao Wang(王慧超)[1*]

[1]*Guangdong Provincial Key Laboratory of Magnetoelectric Physics and Devices, School of Physics, Sun Yat-sen University, Guangzhou 510275, China*
[2]*State Key Laboratory of Optoelectronic Materials and Technologies, School of Physics, Sun Yat-sen University, Guangzhou 510275, China*

(Received 16 May 2023; accepted manuscript online 22 May 2023)

Temperature-driven change of Fermi surface has been attracting attention recently as it is fundamental and essential to understand a metallic system. We report the magnetotransport anomalies in the semimetal $HfTe_2$ single crystals. The magnetoresistance behavior at high temperatures obeys Kohler's rule which can lead to the field-induced resistivity upturn behavior as observed. When the temperature is decreased to around 30 K, Kohler's rule becomes inapplicable, indicating the change of the Fermi surface in $HfTe_2$. The Hall analyses and extended Kohler's plot reveal abrupt change of carrier densities and mobilities near 30 K. These results suggest that the chemical potential may shift as the temperature increases and the shift causes an electron pocket to vanish. Our work of the temperature-driven Lifshitz transition in $HfTe_2$ is relevant to understanding of the transport anomalies and exotic physical properties in transition-metal dichalcogenides.

DOI: 10.1088/0256-307X/40/6/067101

Lifshitz transition is a fundamental phase transition involving change of Fermi surface topology.[1] Since Fermi surface is at the heart of understanding metals, its abrupt change can lead to fantastic phenomena such as superconductivity. Hence the study of Lifshitz transition is of broad interest and significance. Lifshitz transition has been demonstrated in a wide range of materials,[2–6] in which the driven factors can be chemical doping, pressure, magnetic field, and so on. Recently, a novel type of temperature-induced Lifshitz transition has become a compelling research topic, particularly in topological materials.[7,8] It is crucial to understand the anomalous temperature-dependent properties and the physical origin which calls for more experimental results in different systems.

Layered transition-metal dichalcogenide (TMD) hafnium ditelluride has gained increasing attention as a candidate for topological semimetal recently.[9–12] The material possesses semimetallic electronic structure with both electron and hole pockets at or in the vicinity of the Fermi level, which were confirmed by experimental results of angle-resolved photoemission spectroscopy (ARPES) at low temperatures.[11,13] Topological feature such as the occurrence of bulk Dirac point was detected in the system[9,13] though the transport measurements do not provide strong evidence. The disparity may be due to the Fermi level that is far away from the Dirac point. The electronic structure of $HfTe_2$ can be properly tuned by various external parameters. For example, a phase transition appears in high pressure.[10] A dimensionality reduction from 3D (dimensional) to 2D electronic states and band quantization are induced by potassium intercalation effect.[11,13] The $HfTe_2$ exhibits notable temperature-dependent carriers and transport behavior,[10] while the underlying physics has not yet been fully understood.

In this Letter, we report the transport signatures of temperature-driven change of the Fermi surface in $HfTe_2$ single crystals. The analyses of the measured magnetoresistance (MR) results reveal that Kohler's rule is obeyed well at high temperatures while it becomes invalid as the temperature drops to around 30 K. Meanwhile, the unsaturated quadratic MR is largely elevated at low temperatures. In addition, a crossover from linear to nonlinear Hall traces is observed around 30 K where both the carrier density and mobility show anomalous change. These transport features suggest the change of the Fermi surface induced by the shift of the chemical potential as temperature varies. The temperature-driven Lifshitz transition can be an important mechanism to be taken into consideration for understanding the temperature-dependent properties of similar TMDs.

$HfTe_2$ has layered structure and crystallizes in the trigonal $P\bar{3}m1$ space group [Fig. 1(a)].[14] The $HfTe_2$ sheets are stacked along the (001) direction. The studied $HfTe_2$ crystals were grown by Te-flux method avoiding introducing other impurities.[15] The total elements mass of 5 g (Hf, 99.99%, Zr < 0.03%; Te, 99.9999%) with a Hf/Te ratio of about 5 : 95 was loaded in a quartz tube. Tubes were sealed with a pressure less than 5×10^{-4} mbar. Then the tubes were heated to 1000 ℃ within 16 h, held for 24 h, and cooled with a rate of 2 ℃/h to 700 ℃ to remove the flux by a centrifuge. The obtained single crystals are intrinsically

*Corresponding author. Email: wanghch26@mail.sysu.edu.cn
© 2023 Chinese Physical Society and IOP Publishing Ltd

gold in color [Fig. 1(b) inset] with layered structures. The typical sample size is about $2 \times 1 \times 0.1\,\mathrm{mm}^3$. The samples are extremely sensitive in the atmosphere and a dark grey oxide film forms on the surface within several hours. Hence the crystals were kept in the glove box before measurements to protect them from air and moisture.

The as-synthesized crystals were characterized by energy dispersive spectrometry (EDS) collected by a BRUKER x-ray energy spectrometer on a Zeiss scanning electron microscope (EVO MA10). The x-ray diffraction (XRD) spectrum was measured by a PANalytical Empyrean 2 diffractometer where x-ray was excited by a copper target with a wavelength of 1.54 Å. The transport measurements were performed in a 14 T-PPMS (Physical Property Measurement System, Quantum Design) with standard four-probe or six-probe method. Silver epoxy was used to paste the gold wires to the crystals. Since $HfTe_2$ is easily oxidized, we scraped off the top layer to obtain the golden fresh surface before putting the silver glue on the sample. After finishing the preparation of the electrodes, the samples were put into PPMS soon to be vacuumed and the intrinsic properties were detected.

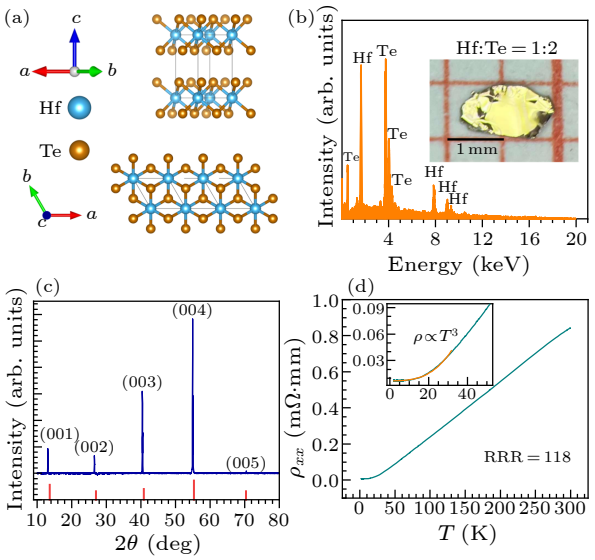

Fig. 1. (a) Crystal structure of $HfTe_2$. (b) EDS spectrum showing a Hf:Te ratio close to 1:2. (c) XRD results of $HfTe_2$ indicating the c-axis along the normal direction of the crystal plane. (d) Temperature-dependent resistivity under zero magnetic field. Inset: the resistivity at low temperature, obeying $\rho = \rho_0 + AT^3$, indicating dominant s–d interband scattering in the material.

The EDS results [Fig. 1(b)] characterize the as-synthesized crystals to be $HfTe_2$ with a Hf:Te ratio close to 1:2. The XRD pattern [Fig. 1(c)] shows that the $(00n)$ diffraction peaks agree well with those of $HfTe_2$. The zero-field resistivity versus temperature curve [Fig. 1(d)] of $HfTe_2$ reveals a typical metallic characteristic. At high temperature, the resistivity is linearly dependent on temperature ($\rho \sim T$) originating from the electron-phonon coupling. A deviation from linear behavior occurs at around 50 K and the resistivity transits to $\rho \sim T^3$ at lower temperatures. The low temperature resistivity of a metal can be usually expressed as $\rho = \rho_0 + AT^n$ with n depending on the particular material. The $n = 2$ indicates dominant electron-electron scattering mechanism. The $n = 3$ behavior is related to the so-called Bloch–Wilson limit and is generally observed in transition-metal compounds as the result of electron-phonon interband scattering referred to as s–d scattering.[16]

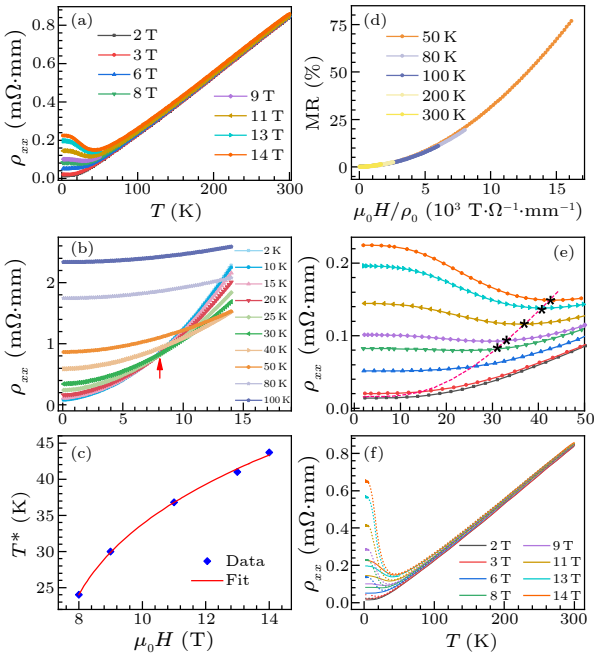

Fig. 2. (a) The temperature-dependent resistivity at different fixed magnetic field perpendicular to the (001) plane. (b) The magnetoresistivity showing cross behavior below 30 K. (c) Magnetic field dependence of the crossover temperature T^*. (d) The Kohler plot of the MR at high temperatures. (e) Magnification of (a) below 50 K. The five black stars denote the resistivity minima and the pink dashed line highlights the location of the resistance minima induced by $\rho(T^*, 0) = [1 + (m - 1)^{-1}] \cdot \rho(T, 0)$. (f) The field-induced resistivity upturn shows discrepancy from the prediction of $\rho_{xx}(T, H) = \rho(T,0) + \alpha \cdot H^m/[\rho(T, 0)]^{m-1}$, which describes the MR obeying Kohler's rule. The dotted lines are the calculations and the solid lines are the experimental results.

With the application of a magnetic field, the resistivity shows an upturn and transition into plateaus at low temperatures when the field ($H//c$-axis) is above 6 T [Fig. 2(a)]. The current is always applied along a-axis and the magnetic field is always perpendicular to the ab plane, i.e., along c-axis in this work. In addition, the MR curves at fixed low temperatures (below 30 K) exhibits a "cross-point" at round 7.5 T [Fig. 2(b)]. It is found that the upturn is induced by magnetic field, different from the zero-field resistivity upturn by electron-electron interaction or weak localization.[17,18] The field-induced metal-insulator-transition-like behavior was observed in a wide range of materials with large MR effect and the origin is under debate.[19–23] The similar phenomenon in graphite was attributed to the occurrence of an excitonic gap in the linear spectrum of the Coulomb interacting quasiparticles,[20] and this mechanism has been widely used to discuss the origin of the metal-insulator-transition-like behavior. In fact, the insulating-like behavior at low temperature is

not necessarily related to a gap as demonstrated in Sb.[24] Thus, though an opening gap can be estimated from the resistivity upturn according to the thermal activated transport theory as in the case of an intrinsic semiconductor, no concrete evidences support the existence of a real band gap in $HfTe_2$.

A plausible explanation of the resistivity upturn behavior is the large MR effect obeying Kohler's rule, a classical description of MR which expresses MR, due to an applied magnetic field H, as a scaling function of (H/ρ_0),[19] i.e.,

$$\mathrm{MR} = \alpha \cdot [H/\rho(T,0)]^m, \tag{1}$$

where α and m are two parameters. In this case, the field resistivity at different temperatures can be expressed as

$$\rho_{xx}(T,H) = \rho(T,0) + \alpha \cdot H^m/[\rho(T,0)]^{m-1}, \tag{2}$$

in which the second term induced by magnetic field competes with the first term when temperature is changed and results in a minimum at the crossover temperature T^*. Equation (2) explains the resistivity plateaus below 10 K at fixed magnetic fields when the parameters α and m are constant and the zero-field $\rho(T,0)$ is nearly unchanged at low temperatures. The formula also predicts that the resistivity at the minimum of the $\rho_{xx}(T,H)$ curve satisfies $d\rho_{xx}(T,H)/dT = 0$, which yields

$$\rho(T^*,0) = H \cdot [\alpha \cdot (m-1)]^{1/m}. \tag{3}$$

Since the resistivity minima occur in the temperature regime where the temperature dependence of the zero-field resistivity follows $\rho = \rho_0 + AT^3$, we obtain $T^* \sim (H - H_c)^{1/3}$ with $H_c = \rho_0 \cdot [\alpha \cdot (m-1)]^{-1/m}$. We plot T^* versus H in Fig. 2(c) and the fit of $T^* \sim (H - H_c)^{1/t}$ obtains a parameter with $t = 3$, which is in good agreement with the T^3-dependent zero-field resistivity of $HfTe_2$ at low temperatures. The $T^* \sim H^{1/3}$ characteristic in our results excludes the metal-insulator transition or other gap-opened model in which T^* is expected to follow $T^* \sim H^{1/2}$,[20] and provides support for Kohler's rule of MR to account for the field-induced resistivity upturn behavior in $HfTe_2$ crystals. Figure 2(d) illustrates the Kohler plot of $\mathrm{MR} = [R(H) - R(0)]/R(0)$ at fixed temperatures above 30 K and the MR versus (H/ρ_0) curves collapse into a single one indicating the validity of Kohler's rule. The fit of MR by Eq. (1) gives rise to $\alpha = 1.22\times10^{-8}\ (\Omega\cdot\mathrm{mm/T})^{1.9}$ and $m = 1.85$. Equations (2) and (3) predict

$$\rho(T^*,0) = [1 + (m-1)^{-1}] \cdot \rho(T,0). \tag{4}$$

The pink dashed line plots the location of the resistance minima induced by Eq. (4) with $m = 1.85$ [Fig. 2(e)]. It is found that the predicted T^* is well consistent with that in our measurements for $T^* > 30$ K. When the T^* is below 30 K, the field-induced resistivity upturn behavior is absent in the experiments, which is quite different from the results produced by Eq. (4) [Fig. 2(e)]. In addition, the calculated upturn resistivity (dotted lines) by Eq. (2) is much larger than the experimental results at low temperatures [Fig. 2(f)]. Since the MR is notably large at low temperatures indicating a dominate role of the second term in Eq. (2), the weaker upturn reveals a larger $\rho(T,0)$ corresponding to the measured MR [Fig. 2(f)]. This effect can be caused when only partial carriers responsible for the zero-field resistivity show dominant MR effect following Eq. (1) while the others show smaller MR change considering the multiband nature of $HfTe_2$ as demonstrated below.

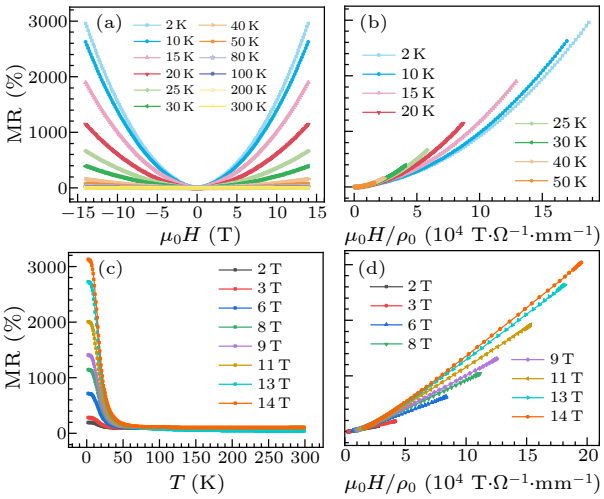

Fig. 3. (a) The MR at selected temperatures. (b) The invalidity of Kohler's rule for the MR in (a) at low temperatures. (c) The temperature-dependent MR at fixed magnetic fields. (d) The MR in (c) showing deviation from Kohler's rule.

The MR curves at different fixed temperatures are obtained from Fig. 2(b) and shown in Fig. 3(a). It is found that the MR largely increases as the temperature is decreased to be below 30 K. The Kohler plot of the MR at low temperatures reveals apparent deviation from Kohler's rule [Fig. 3(b)]. The feature is confirmed by the MR curves at fixed magnetic fields $\mathrm{MR} = [R(T,H) - R(T,0)]/R(T,0)$ [Fig. 3(c)], which do not collapse into one single curve for $\mathrm{MR} \sim H/\rho_0$ [Fig. 3(d)]. The simultaneousness between the invalidity of Kohler's rule and the absence of resistivity upturn behavior demonstrates Kohler's rule accounting for the resistivity upturn. Kohler's rule holds if the number of charge carriers is a constant and the scattering time τ is the same at all points on the Fermi surface.[25] Its validity is illustrated by the temperature and field dependence of MR in many metals. The invalidity of Kohler's rule can be caused by different mechanisms,[25,26] which usually involve the variation of Fermi surface and structure. Since there is no evidence for any structural changes in $HfTe_2$ down to liquid helium temperatures,[27] it is suggested that the deviation from Kohler's rule may not be related to structure change.

We then measured the Hall results [Fig. 4(a)] to explore the temperature dependence of carriers. The Hall trace shows nearly linear dependence on the magnetic field at relatively higher temperatures with a positive Hall coefficient indicating dominance of the holes. As the temperature is decreased to 30 K, the Hall resistance becomes obviously nonlinear. Using a two-band model to analyze the data, we extract the carrier information from the conductivity tensors $\sigma_{xx} = \frac{\rho_{xx}}{\rho_{xx}^2+\rho_{yx}^2}$ and $\sigma_{xy} = \frac{\rho_{yx}}{\rho_{xx}^2+\rho_{yx}^2}$, where ρ_{xx} and ρ_{yx} are the measured longitudinal resistiv-

ity and Hall resistivity, respectively. The carrier mobility μ and density n as functions of temperature are shown in Figs. 4(b) and 4(c), respectively. Both holes and electrons coexist in the sample at low temperatures, consistent with the calculated electronic structure and experiments.[13] The hole and electron densities estimated from σ_{xy} show only slight deviation from compensation as reported,[10] while the results from σ_{xx} are different, revealing obvious discrepancy between the densities of holes and electrons. This may be because the two-band model analysis alone does not quantitatively determine the carriers in a multiband semimetal.[28] Determining whether $HfTe_2$ is a compensated semimetal actually needs more efforts in the future. Nevertheless, the temperature dependence of the carriers estimated from σ_{xx} and σ_{xy} is well consistent below 30 K, showing increased mobility and carrier density with decreased temperature.

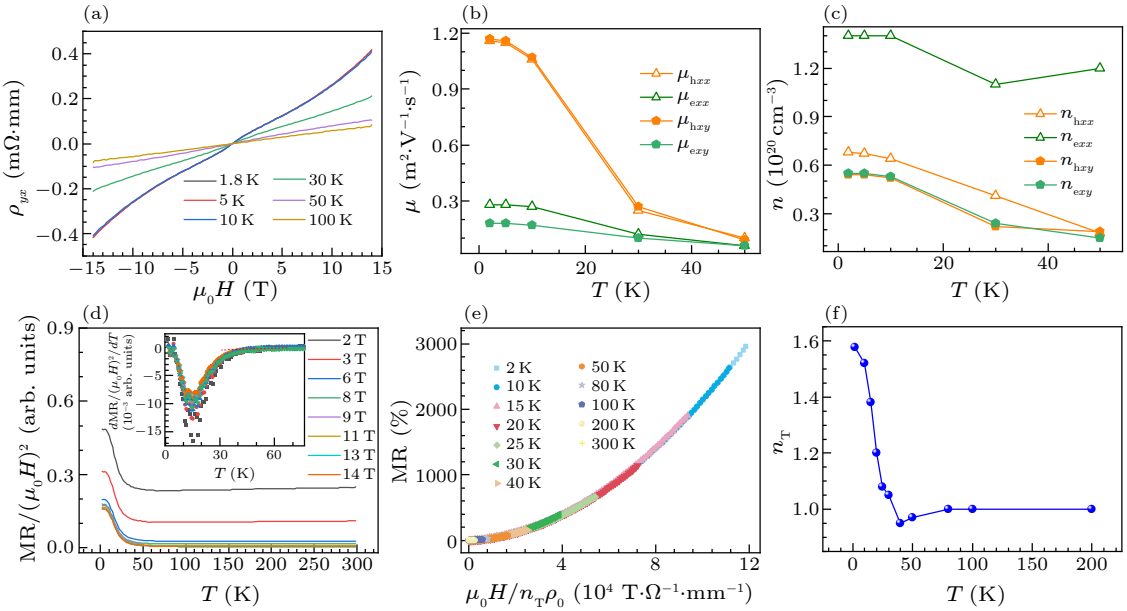

Fig. 4. (a) Hall results at different temperatures. The estimated carrier (b) mobility and (c) density as a function of temperature. (d) A plot of $\mathrm{MR}/(\mu_0 H)^2$ revealing the change of mobility with temperatures. Inset: the differential results indicating the increase of mobility at around 30 K. (e) The extended Kohler plot of the MR curves with n_T describing the change of carrier density with temperature. (f) The temperature-dependent n_T derived from (e).

It is found the mobility dependence on the temperature [Fig. 4(b)] is similar to the change of MR versus temperature at a fixed magnetic field. This can be explained by Eq. (2) where constants α and m are insensitive to temperature, and the temperature dependence of the MR in a fixed magnetic field is only determined by $\rho(T, 0)$. Moreover, $\rho(T, 0)$ is inversely proportional to the mobilities $\mu_{\mathrm{e,h}}(T)$. The higher mobility thus leads to a larger MR when the second term dominates in Eq. (2). In addition, we plot the MR/H^2 versus temperature at different fields [Fig. 4(d)], which reflects the change of mobility. The differential results are shown in the inset of Fig. 4(d) and reveal that the MR/H^2 sharply increases at around 30 K, well consistent with the Hall analyses. Thus, the large MR behavior in $HfTe_2$ can be mainly attributed to the rise of carrier mobility at low temperatures. The underlying origin of the large residual-resistivity-ratio (RRR) values, ultra-high mobilities and a non-saturating MR is usually ascribed to be related to the topological protection in a topological material.[29] We note that the current experimental results do not provide concrete evidences for the $HfTe_2$ as a topological semimetal and the calculated Dirac point is far away from the Fermi level, which means that the topological protection may not play an important role in the transport phenomena.

As discussed above, the deviation of Kohler's rule originates from that the MR at low temperature is smaller than the expected value for Kohler's rule. The MR can be analyzed by the extended Kohler plot $\mathrm{MR} \sim H/(n_\mathrm{T}\rho_0)$ to collapse into one single curve [Fig. 4(e)], in which n_T describes the change of carrier density with temperature.[30] With n_T defined as 1 at 300 K, n_T is about 1 at high temperatures and increases from about 30 K to the largest $n_\mathrm{T} \approx 1.6$ at 2 K [Fig. 4(f)]. Obviously, the temperature dependence of n_T cannot be attributed to the thermally induced change in the carrier density which should change pronouncedly at high temperatures.[28] The $n_\mathrm{T} > 1$ indicates that the zero-field resistivity $\rho_1 = n_\mathrm{T}\rho$ corresponding to the observed MR is actually larger than the measured ρ. The discrepancy can be explained by the appearance of another conduction channel with $1/\rho = 1/\rho_1 + 1/\rho_2$. The magnetoresistivity then satisfies $1/\rho(H) = 1/\rho_1(H) + 1/\rho_2(H)$. The measured $\mathrm{MR} = [\rho(H) - \rho(0)]/\rho$ would be smaller than the expected $\mathrm{MR}_1 = [\rho_1(H) - \rho_1(0)]/\rho_1$ when another conduction channel contributes a smaller MR. Thus, the temperature dependence of n_T suggesting the appearance of a new conduction channel at low temperatures provides support for the Lifshitz transition in $HfTe_2$.

The carrier density estimated from both σ_{xx} and σ_{xy} is shown to be increased below 30 K, in good agreement

with the temperature dependence of $n_{\rm T}$, which confirms the feature as an intrinsic property in the semimetal. The first-principles band-structure calculations reveal the semimetallic nature of bulk $HfTe_2$, showing two hole pockets crossing the Fermi level $E_{\rm F}$ at the Γ point and an electron pocket around the M and L point.[10,13] The ARPES experiments confirm the coexistence of hole and electron pockets at low temperatures,[11,13] which is consistent with our transport results at low temperatures. At high temperatures, however, only holes are derived from our 100 K Hall analyses and the obtained electron density from 50 K data is fragile, depending on parameter initialization. Based on the calculated electronic structure,[13] the electron pocket may not cross the Fermi level if the chemical potential shifts downwards. Thus, the disappearance of electron information at high temperatures suggests the possible shift of the chemical potential. At high temperatures above 50 K, it seems that there are only two hole pockets cross the Fermi level at the Γ point. Since the two Fermi pockets both come from the Te $5p$ orbital, their scattering mechanisms can be similar and Kohler's rule holds. When the temperature is decreased to 30 K, the appearance of considerate electron pocket from Hf $5d$ orbital introduce a different scattering time, and thus the MR behavior deviates from Kohler's rule. A change of hole density is expected when the chemical potential is just touching the electron, and signatures are observed in the $n_{\rm hole}$ estimated from σ_{xx} and the decrease of $n_{\rm T}$ around 50 K. The further increase of holes with decreased temperature may be caused by the requirement of compensation in a semimetal.[31] Similar temperature-driven Lifshitz transition was reported in the TMD WTe_2 and the electronic structure calculations suggest that the shift of the chemical potential with temperature, responsible for the Lifshitz transition, is caused by the close proximity of electron and hole densities of states near the Fermi energy.[7] The mechanism may be applicable to the similar semimetallic TMD system $HfTe_2$. However, we do not have a clear answer on the origin yet, and there may be some deep physical mechanism that calls for further investigations. The change of the Fermi surface can be directly verified by the temperature-dependent ARPES measurements in future and more efforts are needed to fully understand the occurrence of the temperature-driven Lifshitz transition in TMDs.

In summary, we report the field-induced resistivity upturn, invalid and valid Kohler's rule, and Hall behavior of $HfTe_2$ single crystals, in which the transport anomalies may be related to the temperature-driven Lifshitz transition. The MR behavior at high temperatures follows Kohler's rule, which qualitatively accounts for the field-induced resistivity upturn behavior. As the temperature is decreased to about 30 K, the abrupt deviation of Kohler's rule and the nonlinear Hall resistance indicate the change of the Fermi surface in $HfTe_2$. The Hall analyses and extended Kohler plot reveal the obvious change of carrier densities and mobilities near 30 K. The results can be caused if the chemical potential shifts with increased temperature involving the disappearance of an electron pocket. The study of the temperature-driven Lifshitz transition provides insights into the understanding of the temperature-dependent exotic phenomena in TMDs.

Acknowledgments. This work was supported by the National Natural Science Foundation of China (Grant Nos. 21BAA01133, 12004441, 92165204, 11974431, 11774434, and U2130101), the Natural Science Foundation of Guangdong Province of China (Grant No. 2023A1515010487), the Guangzhou Basic and Applied Basic Research Foundation (Grant No. 202201011109), and the Fundamental Research Funds for the Central Universities (Grant No. 22hytd07).

References

[1] Lifshitz I M 1960 *Sov. Phys. JETP* **11** 1130
[2] Xiang Z J, Ye G J, Shang C, Lei B, Wang N Z, Yang K S, Liu D Y, Meng F B, Luo X G, Zou L J, Sun Z, Zhang Y, and Chen X H 2015 *Phys. Rev. Lett.* **115** 186403
[3] Liu Y Y, Liu Y F, Gui X, and Jia S 2020 *Proc. Natl. Acad. Sci. USA* **117** 15517
[4] Liu C, Kondo T, Fernandes R M, Palczewski A D, Mun E D, Ni N, Thaler A N, Bostwick A, Rotenberg E, Schmalian J, Bud'ko S L, Canfield P C, and Kaminski A 2010 *Nat. Phys.* **6** 419
[5] Zhang Y, Wang C L, Yu L, Liu G D, Liang A J, Huang J W, Nie S M, Sun X, Zhang Y X, Shen B, Liu J, Weng H M, Zhao L X, Chen G F, Jia X W, Hu C, Ding Y, Zhao W J, Gao Q, Li C, He S L, Zhao L, Zhang F F, Zhang S J, Yang F, Wang Z M, Peng Q J, Dai X, Fang Z, Xu Z Y, Chen C T, and Zhou X J 2017 *Nat. Commun.* **8** 15512
[6] Beaulieu S, Dong S, Tancogne-Dejean N, Dendzik M, Pincelli T, Maklar J, Xian R P, Sentef M A, Wolf M, Rubio A, Rettig L, and Ernstorfer R 2021 *Sci. Adv.* **7** eabd9275
[7] Wu Y, Jo N H, Ochi M, Huang L, Mou D, Bud'ko S L, Canfield P C, Trivedi N, Arita R, and Kaminski A 2015 *Phys. Rev. Lett.* **115** 166602
[8] Chen F C, Fei Y, Li S J, Wang Q, Luo X, Yan J, Lu W J, Tong P, Song W H, Zhu X B, Zhang L, Zhou H B, Zheng F W, Zhang P, Lichtenstein A L, Katsnelson M I, Yin Y, Hao N, and Sun Y P 2020 *Phys. Rev. Lett.* **124** 236601
[9] Aminalragia-Giamini S, Marquez-Velasco J, Tsipas P, Tsoutsou D, Renaud G, and Dimoulas A 2017 *2D Mater.* **4** 015001
[10] Mangelsen S, Naumov P G, Barkalov O I, Medvedev S A, Schnelle W, Bobnar M, Mankovsky S, Polesya S, Näther C, Ebert H, and Bensch W 2017 *Phys. Rev. B* **96** 205148
[11] Nakata Y, Sugawara K, Chainani A, Yamauchi K, Nakayama K, Souma S, Chuang P Y, Cheng C M, Oguchi T, Ueno K, Takahashi T, and Sato T 2019 *Phys. Rev. Mater.* **3** 071001
[12] Wang Y Y, Guo P J, Xu S, Liu K, and Xia T L 2020 *Phys. Rev. B* **101** 035145
[13] El Youbi Z, Jung S W, Mukherjee S, Fanciulli M, Schusser J, Heckmann O, Richter C, Minár J, Hricovini K, Watson M D, and Cacho C 2020 *Phys. Rev. B* **101** 235431
[14] Momma K and Izumi F 2011 *J. Appl. Crystallogr.* **44** 1272
[15] Mangelsen S and Bensch W 2020 *Inorg. Chem.* **59** 1117
[16] Wilson A H 1938 *Proc. R. Soc. Lond. A* **167** 580
[17] Li C S, Boubeche M, Zeng L Y, Ji Y, Li Q X, Guo D H, Zhu Q Z, Zhong D Y, Luo H X, Wang H C 2022 *Phys. Status Solidi RRL* **16** 2100650
[18] Wang J, DaSilva A M, Chang C Z, He K, Jain J K, Samarth N, Ma X C, Xue Q K, and Chan M H W 2011 *Phys. Rev. B* **83** 245438
[19] Wang Y L, Thoutam L R, Xiao Z L, Hu J, Das S, Mao Z Q, Wei J, Divan R, Luican-Mayer A, Crabtree G W, and Kwok W K 2015 *Phys. Rev. B* **92** 180402
[20] Khveshchenko D V 2001 *Phys. Rev. Lett.* **87** 206401
[21] Du X, Tsai S W, Maslov D L, and Hebard A F 2005 *Phys. Rev. Lett.* **94** 166601
[22] Zhao Y F, Liu H W, Yan J Q, An W, Liu J, Zhang X, Wang H C, Liu Y, Jiang H, Li Q, Wang Y, Li X Z, Mandrus D, Xie X C, Pan M, and Wang J 2015 *Phys. Rev. B* **92** 041104

[23] Tafti F F, Gibson Q D, Kushwaha S K, Haldolaarachchige N, and Cava R J 2016 *Nat. Phys.* **12** 272
[24] Li Z, Li G, Wang N L, and Luo J L 2008 *J. Phys.: Condens. Matter* **20** 235232
[25] McKenzie R H, Qualls J S, Han S Y, and Brooks J S 1998 *Phys. Rev. B* **57** 11854
[26] Harris J M, Yan Y F, Matl P, Ong N P, Anderson P W, Kimura T, and Kitazawa K 1995 *Phys. Rev. Lett.* **75** 1391
[27] Klipstein P C, Guy D R P, Marseglia E A, Meakin J I, Friend R H, and Yoffe A D 1986 *J. Phys. C: Solid State Phys.* **19** 4953
[28] Xu J, Wang Y, Pate S E, Zhu Y L, Mao Z Q, Zhang X F, Zhou X Q, Welp U, Kwok W K, Chung D Y, Kanatzidis M G, and Xiao Z L 2023 *Phys. Rev. B* **107** 035104
[29] Kumar N, Sun Y, Xu N, Manna K, Yao M, Süss V, Leermakers I, Young O, F T, Schmidt M, Borrmann H, Yan B, Zeitler U, Shi M, Felser C, and Shekhar C 2017 *Nat. Commun.* **8** 1642
[30] Xu J, Han F, Wang T T, Thoutam L R, Pate S E, Li M D, Zhang X F, Wang Y L, Fotovat R, Welp U, Zhou X Q, Kwok W K, Chung D Y, Kanatzidis M G, and Xiao Z L 2021 *Phys. Rev. X* **11** 041029
[31] Thoutam L R, Pate S E, Wang T T, Wang Y L, Divan R, Martin I, Luican-Mayer A, Welp U, Kwok W K, and Xiao Z L 2022 *Phys. Rev. B* **106** 155117